Human invariant natural killer T cells acquire transient innate responsiveness via histone H4 acetylation induced by weak TCR stimulation

Xiaohua Wang,[1] Kathleen A. Bishop,[3] Subramanya Hegde,[1] Lance A. Rodenkirch,[2] J. Wesley Pike,[3] and Jenny E. Gumperz[1]

[1]Department of Medical Microbiology and Immunology and [2]W.M. Keck Laboratory for Biological Imaging, School of Medicine and Public Health and [3]Department of Biochemistry, University of Wisconsin-Madison, Madison, WI 53706

Invariant NKT cells (iNKT cells) are innate T lymphocytes that are thought to play an important role in producing an early burst of IFN-γ that promotes successful tumor immunosurveillance and antimicrobial immunity. The cellular activation processes underlying innate IFN-γ production remain poorly understood. We show here that weak T cell receptor (TCR) stimulation that does not directly activate iNKT cell IFN-γ messenger RNA transcription nevertheless induces histone H4 acetylation at specific regions near the *IFNG* gene locus. This renders the iNKT cells able to produce IFN-γ in an innate manner (i.e., not requiring concurrent TCR stimulation) upon exposure to IL-12 and IL-18. The iNKT cells retain the capacity for innate activation for hours to days after the initial weak TCR stimulation, although their innate responsiveness gradually declines as a function of histone deacetylation. These results explain how iNKT cells are able to mediate rapid innate IFN-γ secretion in a manner that does not require them to undergo permanent T_{H1} differentiation. Moreover, our results also indicate that iNKT cell motility is maintained during activation by IL-12 and IL-18. Therefore, iNKT cells activated through this pathway can continue to migrate and may thus disseminate the IFN-γ that they produce, which may amplify its impact.

CORRESPONDENCE
Jenny E. Gumperz:
jegumperz@wisc.edu

Abbreviations used: α-GalCer, α-galactosylceramide; ChIP, chromatin immunoprecipitation; CsA, cyclosporin A; ERK, extracellular signal-regulated kinase; HAT, histone acetyl transferase; HDAC, histone deacetylase; iNKT cell, invariant NKT cell; MAPK, mitogen-activated protein kinase; mRNA, messenger RNA; TSA, trichostatin A.

The cytokine IFN-γ plays a central role in the induction of cell-mediated immune responses that provide protection against many viral and bacterial infections and that lead to the eradication of nascent neoplastic cells. Production of IFN-γ occurs in successive stages during immune responses. Innate lymphocytes, which are present from birth and are activated by evolutionarily conserved mechanisms, are thought to be critical for producing an initial burst of IFN-γ that helps to drive the activation of adaptive T lymphocytes that then produce the cytokine in response to stimulation by specific foreign antigens. Subsequently, T_{H1}-polarized effector and memory T cells can produce large quantities of IFN-γ in a TCR-independent manner in response to cytokines such as IL-12 and IL-18. Although the cellular and genetic processes involved in the differentiation of adaptive T lymphocytes into effector and memory cells specialized for IFN-γ production are becoming comparatively well understood (Fitzpatrick and Wilson, 2003; Reiner et al., 2003), the processes responsible for the ability of innate lymphocytes to deliver the initial burst of IFN-γ are less clear.

Invariant NKT cells (iNKT cells) are innate T lymphocytes that have been observed to be among the first cells producing IFN-γ in microbial infections (Brigl et al., 2003). IFN-γ production by iNKT cells has also been shown to be critical for successful immunosurveillance of certain types of tumors in mice (Crowe et al., 2002). iNKT cells can be activated to produce

X. Wang's present address is Dept. of Cell Biology, Albert Einstein College of Medicine, Bronx, NY 10461.
K.A. Bishop's present address is Maine Medical Center Research Institute, Scarborough, ME 04074.
S. Hegde's present address is Dept. of Surgery, School of Medicine and Public Health, University of Wisconsin-Madison, Madison, WI 53792.

The Rockefeller University Press $30.00
J. Exp. Med. Vol. 209 No. 5 987-1000
www.jem.org/cgi/doi/10.1084/jem.20111024

The Journal of Experimental Medicine

IFN-γ in two ways: (1) via TCR stimulation and (2) via signaling through cell surface receptors for cytokines such as IL-12, IL-18, and IFN-α. TCR-mediated activation of iNKT cells occurs as a result of the recognition of specific lipids presented as antigens by CD1d molecules expressed on APCs. The lipid antigens recognized by iNKT cells include certain types of foreign glycolipids (e.g., α-linked glycosphingolipids), as well as specific self-lipids such as lysophosphatidylcholine and particular forms of β-D-glucopyranosylceramide (Kawano et al., 1997; Kinjo et al., 2005; Mattner et al., 2005; Fox et al., 2009; Brennan et al., 2011). Whether an iNKT cell produces IFN-γ in response to TCR signaling depends in part on the strength of the TCR stimulation received. Activation of iNKT cells by the synthetic compound α-galactosylceramide (α-GalCer), which is a strong TCR agonist, produces a robust cytoplasmic calcium flux and leads to the production of IFN-γ as well as other cytokines (e.g., GM-CSF, IL-13, IL-4, and IL-2). In contrast, activation of iNKT cells by CD1d molecules expressed on APCs resembled signaling from a weak TCR stimulus, in that there was little detectable cytoplasmic calcium flux, and resulted mainly in secretion of GM-CSF and IL-13 (Wang et al., 2008a). Thus, autoantigenic stimulation of iNKT cells by $CD1d^+$ APCs probably does not usually provide a strong enough TCR signal to induce substantial IFN-γ production.

However, during inflammation, iNKT cells are prominent early producers of IFN-γ. A recent analysis has demonstrated that iNKT cell production of IFN-γ during diverse bacterial infections is highly dependent on the presence of IL-12, regardless of whether or not the bacteria expressed compounds that are recognized as antigens by the iNKT cells (Brigl et al., 2011). This finding underscores the fact that IFN-γ production by iNKT cells is not dependent on foreign antigens and that the cytokine-mediated pathway probably represents their dominant means of activation in most physiological contexts. Yet, the role of autoantigenic TCR signaling in IL-12–induced IFN-γ production by iNKT cells has been unclear. In initial studies exploring iNKT cell IFN-γ production in microbial infections, their responses to proinflammatory cytokines appeared to be dependent on TCR-mediated recognition of self-antigens (Brigl et al., 2003; Mattner et al., 2005). However, in subsequent analyses, it appeared that iNKT cells could produce IFN-γ in response to cytokines such as IL-12, IL-18, and IFN-α even when a TCR signal was not present (Nagarajan and Kronenberg, 2007; Tyznik et al., 2008; Wesley et al., 2008).

In investigating the requirements for IFN-γ production by iNKT cells, we found that a transient exposure of iNKT cells to $CD1d^+$ APCs rendered them subsequently able to produce IFN-γ in response to IL-12 and IL-18 alone, whereas rested iNKT cells that had not recently been exposed to antigenic stimulation showed no IFN-γ secretion in response to these cytokines (Wang et al., 2008a). Thus, it seems that although the TCR signals produced by recognition of cellular antigens are often not strong enough to directly induce iNKT cell IFN-γ production, this stimulation does produce an altered state in which the iNKT cells are able to respond to proinflammatory cytokines without requiring concurrent TCR signaling. This observation raises intriguing questions about how the initial TCR signal might be biochemically stored within the iNKT cell so as to enable later responses to cytokine receptor stimulation. In this study, we have investigated this question. Our results show that autoantigenic activation of iNKT cells induces increased acetylation of histone H4 at the *IFNG* locus that is not associated with immediate gene transcription. However, the increased histone acetylation provides for a window of time in which transcription of IFN-γ messenger RNA (mRNA) can be initiated by cytokine receptor signaling that would otherwise be nonproductive. That iNKT cells retain their cellular motility during this pathway of IFN-γ production suggests that they can migrate away from sites of activation before delivering their cytokine payload. This continued motility may therefore allow iNKT cells to disseminate IFN-γ to nearby cell populations that have not yet received microbial stimulation, which may provide for improved containment of the infection.

RESULTS

To confirm that primary human iNKT cells are able to produce IFN-γ in an innate manner similar to what we have observed previously using cultured human iNKT cells (Wang et al., 2008a), we isolated human PBMCs and removed the cell types that express CD1d (i.e., monocytes, B cells, and DCs) and then exposed the remaining cells to a mixture of IL-12, IL-18, and IFN-α. We observed that a fraction of the iNKT subset was able to produce IFN-γ in response to the proinflammatory cytokines (Fig. 1 A). The fraction of the iNKT cells that showed IFN-γ staining was comparable with that in the NK cell–enriched population and was significantly greater than that of the other T cells (Fig. 1 B). Most of the primary iNKT cells lost their cytokine-induced IFN-γ response over the course of a 3–5-d incubation in the absence of $CD1d^+$ APCs, although they largely retained the capacity to produce IFN-γ in response to PMA and ionomycin, drugs which mimic strong TCR signaling (Fig. 1 C). NK cells in the same PBMC samples also showed a decline in cytokine-induced IFN-γ production after 3–5 d ex vivo in the absence of APCs; however, the magnitude of the decline was greater for the iNKT cells (Fig. 1 D). These results suggested that a fraction of the iNKT cells in human peripheral blood are in a reversible state of innate responsiveness.

Because it is not possible to create an in vivo model system in which IL-12 and autoantigenic TCR signaling can be temporally segregated, to further investigate the mechanisms involved in this state, we set up an in vitro system that would allow us to separate the timing of these two kinds of stimulation. As a source of iNKT cells, we used human iNKT cell clones because these cells are not neoplastically transformed, and thus, like T cells in vivo, their cellular activation processes subside if they do not receive continued stimulation. We used human B lymphoblastoid cells transfected with CD1d as APCs because we and others have previously shown that CD1d molecules from this type of cell contain bound lysophosphatidylcholine, a self-lipid which is recognized by human iNKT cells (Cox et al., 2009; Fox et al., 2009; Yuan et al., 2009). The iNKT cells were exposed for 4 h

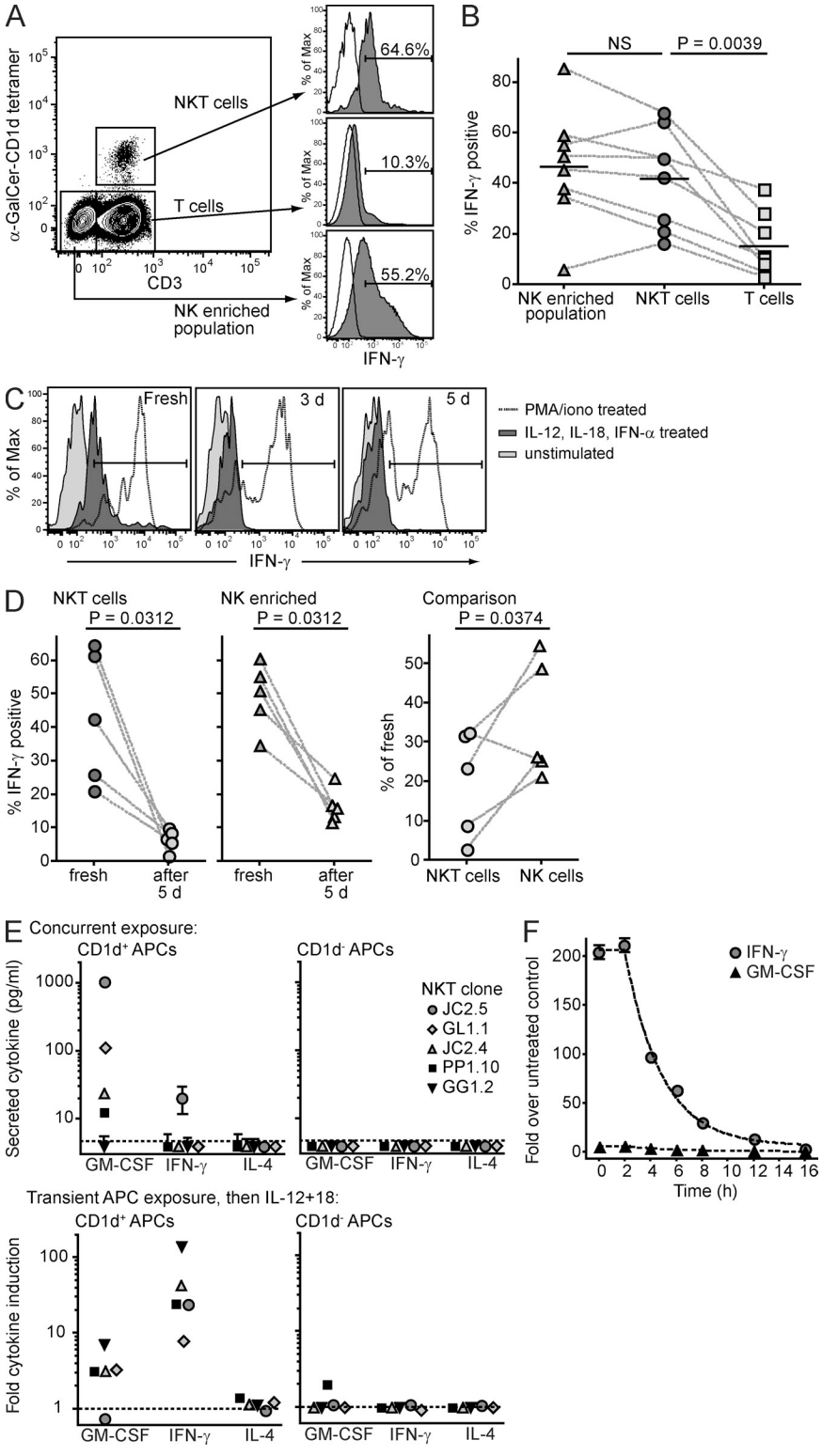

Figure 1. Autoantigenic stimulation primes iNKT cells for subsequent TCR-independent IFN-γ production. (A) Flow cytometric analysis of an experiment in which isolated human PBMCs were depleted of B cells, monocytes, and DCs and then incubated in medium alone (open histograms) or in medium containing a mixture of IL-12, IL-18, and IFN-α (closed histograms). The cells were stained with α-GalCer–loaded CD1d tetramer and anti-CD3 and then fixed, permeabilized, and stained for intracellular IFN-γ. Results shown are from one representative analysis out of eight. (B) Compiled results from analyses of eight different human peripheral blood samples, showing the percentage of the indicated cell populations in each sample that stained positively for IFN-γ after the treatment described in A. Horizontal bars indicate the mean. (C) Flow cytometric analysis showing the intracellular IFN-γ staining of the peripheral blood iNKT cell population of an unstimulated sample (light gray histograms) compared with a sample treated with IL-12, IL-18, and IFN-α (dark gray histograms) or PMA and ionomycin (dotted lines) at the indicated time points. Results are from one representative experiment out of three. (D) Compiled results from analyses of five different human peripheral blood samples for IFN-γ staining induced by IL-12, IL-18, and IFN-α. The first two plots show the fraction of cells positive for IFN-γ in the iNKT or NK-enriched subsets for freshly isolated samples (fresh) compared with that in samples that were rested for 5 d in the absence of APCs and then exposed to the cytokine mixture (after 5 d). The rightmost plot shows the fraction of iNKT cells compared with NK cells in each sample that retained the ability to produce IFN-γ after 5 d. (E) Cultured human iNKT cells are primed to produce innate IFN-γ by transient exposure to CD1d$^+$ APCs. (top) The indicated iNKT clones were incubated with CD1d-transfected (CD1d$^+$) or untransfected (CD1d$^-$) APCs, and production of the cytokines shown on the x axes was quantitated by ELISA. The dashed lines show the limit of detection of the ELISAs (5 pg/ml). (bottom) iNKT clones were exposed to the indicated APCs for 4 h, and then the APCs were removed. The purified iNKT cells were then incubated with CD1d$^-$ APCs in medium containing IL-12 and IL-18, and cytokine secretion was quantitated by ELISA. Results are shown as the fold increase in cytokine production compared with iNKT cells that were not treated with IL-12 and IL-18 (IFN-γ concentrations were typically in the range of 0.2–2 ng/ml; for the purposes of these analyses, cytokine concentrations that were below the limit of detection of the ELISA were arbitrarily assigned a value of 1 pg/ml). The results shown are from a single experiment in which the indicated iNKT cell clones were tested in parallel; similar results were obtained in at least three additional experiments each for clones GG1.2, JC2.4, and PP1.10. Similar results were also obtained in multiple independent experiments using three additional human NKT cell clones (J3N.5, J24N.22, and GL1.4). (F) iNKT cells were exposed to CD1d$^+$ APCs for 4 h, then the APCs were removed, and the iNKT cells were rested in medium for the indicated times and then exposed to IL-12 and IL-18. Results are expressed as the fold increase in cytokine secretion compared with control iNKT cells that were exposed to the APCs but not stimulated with IL-12 and IL-18. The results shown are representative of three independent analyses on two different iNKT cell clones.

to the CD1d-transfected APCs or to the untransfected APCs, which are negative for CD1d. The APCs were then removed, resulting in iNKT cells that were >99.5% pure (Wang et al., 2008a). The purified iNKT cells were then combined with a 1:1 ratio of CD1d$^-$ APCs in plain medium or in medium containing IL-12 and IL-18, and after 16–18 h, the culture supernatants were analyzed for IFN-γ. As shown in Fig. 1 E (top left), exposing several different human iNKT cell clones to CD1d-transfected APCs for 16–18 h induced most of them to secrete clearly detectable amounts of GM-CSF but little or no detectable IFN-γ or IL-4. However, if the CD1d-transfected APCs were removed, and the iNKT cells were then exposed to IL-12 and IL-18, substantial amounts of IFN-γ were secreted (typically in the range of 0.2–2 ng/ml from 5×10^4 iNKT cells in 200 μl of culture medium), whereas there was only a modest induction of GM-CSF and little or no induction of IL-4 (Fig. 1 E, bottom left). If the iNKT cells were preexposed to CD1d$^-$ APCs and then stimulated with IL-12 and IL-18, there was no detectable cytokine secretion (Fig. 1 E, right), indicating that the iNKT cells do not respond productively to IL-12 and IL-18 signaling when they have not recently received a TCR stimulus. Notably, iNKT cell clones for which self-antigens were not strong enough agonists to directly induce secretion of GM-CSF nevertheless also produced IFN-γ if they were exposed to IL-12 and IL-18 after removal of the CD1d-transfected APCs (see clone GG1.2 in Fig. 1 E), suggesting that even very weak TCR stimulation is sufficient to promote the subsequent innate responsiveness. The primed state resulting from exposure to CD1d$^+$ APCs was transitory because iNKT cells that were treated with IL-12 and IL-18 at time points >2 h after removal of the APCs showed a progressive decline in IFN-γ secretion, although some ability to produce IFN-γ in response to IL-12 and IL-18 was maintained for at least 12–16 h after APC removal (Fig. 1 F). These results demonstrate that there is a window of time after autoantigen exposure during which iNKT cells can produce IFN-γ in response to cytokine receptor stimulation alone, and this window lasts a period of hours for cultured human iNKT cells or days for primary human iNKT cells.

We previously established that the response of autoantigen-primed iNKT cells to IL-12 and IL-18 is not inhibited by the addition of an anti-CD1d blocking antibody, suggesting that it is not dependent on a concurrent TCR signal (Wang et al., 2008a). However, because it is a significant concern that the effect we observed might nevertheless be caused by contamination by a small number of CD1d$^+$ APCs, we performed experiments to test the signaling pathways involved. Blocking activation of extracellular signal-regulated kinase (ERK) during the exposure to the CD1d-transfected APCs almost completely abrogated iNKT cell IFN-γ production in response to subsequent IL-12 and IL-18 treatment (Fig. 2 A), whereas blocking this pathway during the IL-12 and IL-18 exposure step only reduced iNKT cell IFN-γ production

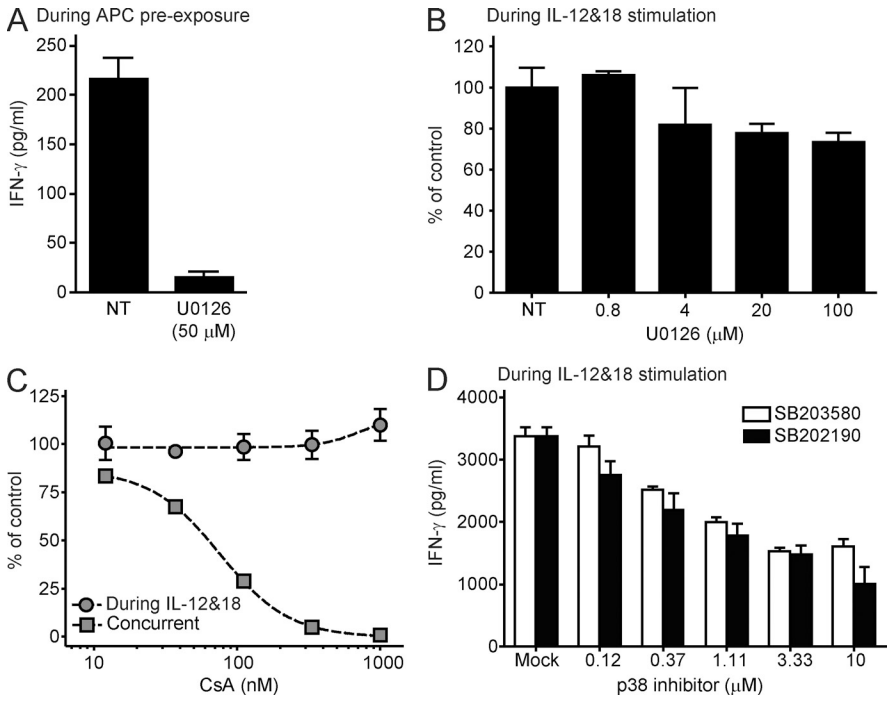

Figure 2. Cytokine-induced IFN-γ production by autoantigen-primed iNKT cells does not require concurrent TCR signaling. (A) Cultured human iNKT cells were exposed to CD1d$^+$ APCs in medium containing 50 μM of the MEK inhibitor U0126 or in medium alone (NT). The APCs and inhibitor were then removed, the iNKT cells were incubated in medium containing IL-12 and IL-18 for 16 h, and IFN-γ secreted into the culture supernatant was quantitated by ELISA. Results are representative of four independent experiments using three different iNKT cell clones. (B) Cultured iNKT cells that had been transiently exposed to CD1d$^+$ APCs were incubated in medium containing IL-12 and IL-18 in the presence or absence of U0126. The plot shows the amount of IFN-γ secreted in the presence of the inhibitor as a percentage of that produced by control iNKT cells stimulated in the absence of U0126 (NT). Results are representative of four independent experiments using three different iNKT cell clones. (C) Effect of CsA on IFN-γ secretion by cultured iNKT cells exposed to IL-12 and IL-18 in the presence of CD1d$^+$ APCs (concurrent) compared with primed iNKT cells during subsequent stimulation with IL-12 and IL-18. The plot shows IFN-γ secretion by treated iNKT cells as a fraction of the amount produced by control iNKT cells that were stimulated in the absence of CsA. Results are representative of four independent experiments using three different iNKT cell clones. (D) Cultured iNKT cells were exposed to CD1d$^+$ APCs, then the APCs were removed, and the iNKT cells were exposed to IL-12 and IL-18 in the presence of the p38 inhibitors SB203580 or SB202190 or the inactive analogue SB202474 (mock). Results are representative of four independent experiments using three different iNKT cell clones. All plots show the means of three replicate samples, with error bars indicating the standard deviations of the means (not always visible on the scales shown).

by 20–30% (Fig. 2 B). Blocking calcium signaling by the addition of cyclosporin A (CsA) during concurrent TCR and IL-12/18 stimulation also abrogated iNKT cell IFN-γ production; however, the addition of CsA to iNKT cells that had been preexposed to CD1d-transfected APCs failed to inhibit the IFN-γ production induced by IL-12 and IL-18 (Fig. 2 C).

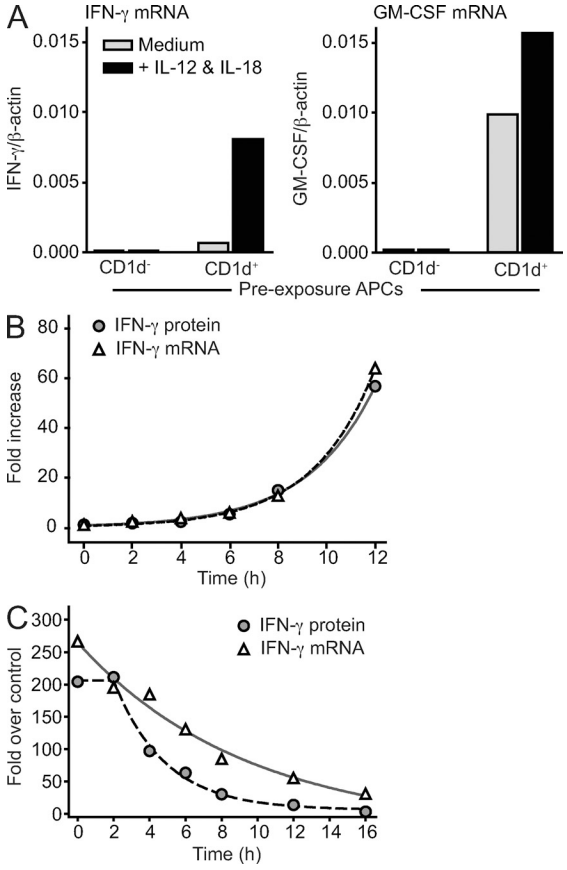

Figure 3. IL-12 and IL-18 stimulation induces IFN-γ mRNA transcription. (A) Real-time PCR analysis of IFN-γ or GM-CSF mRNA from cultured iNKT cells that were transiently exposed to CD1d⁻ or CD1d⁺ APCs and then stimulated with IL-12 and IL-18 or incubated in medium alone. Results are expressed as the signal obtained using IFN-γ or GM-CSF primers, divided by the signal from the same cDNA sample using β-actin primers. The plot shows one representative experiment out of three for a single iNKT cell clone; similar results were also obtained in independent experiments using two additional iNKT cell clones. (B) Kinetics of IFN-γ mRNA and protein production after IL-12 and IL-18 stimulation of cultured iNKT cells that were transiently exposed to CD1d⁺ APCs. Results are expressed as fold increase compared with control iNKT cells that were not stimulated with IL-12 and IL-18. The plot shows one representative experiment out of two; similar results were also obtained in two independent experiments using a different iNKT cell clone. (C) Real-time PCR analysis of IFN-γ mRNA in cultured iNKT cells that were first transiently exposed to CD1d⁺ APCs, then rested for the indicated times, and then stimulated with IL-12 and IL-18. Corresponding measurements of IFN-γ protein secretion from Fig. 2 A are shown for comparison. Results are expressed as fold increase over iNKT cells that were exposed to CD1d⁻ APCs in the first step. The plot shows one representative experiment out of two; similar results were also obtained in two independent experiments using a different iNKT cell clone.

Moreover, addition of specific inhibitors of the p38 mitogen-activated protein kinase (MAPK) during the IL-12 and IL-18 exposure step markedly reduced IFN-γ production (Fig. 2 D), which is consistent with a prior study showing the involvement of p38 MAPK in activation by IL-12 and IL-18 (Yang et al., 2001). Thus, whereas TCR-initiated signals (e.g., ERK phosphorylation and calcium signaling) are involved in the activation by CD1d-transfected APCs, these signals are not required during the subsequent IL-12 and IL-18 activation, and instead this step is more sensitive to p38 MAPK signaling. These observations formally exclude the possibility that our results are simply caused by contaminating CD1d⁺ APCs that continue to provide a TCR signal during the IL-12 and IL-18 exposure step.

A previous study has suggested that mouse iNKT cells store IFN-γ and IL-4 mRNA, enabling them to rapidly translate cytokine proteins (Stetson et al., 2003). However, when we analyzed our human iNKT cell clones, we found that rested cells that had not recently been exposed to CD1d⁺ APCs did not contain detectable levels of IFN-γ mRNA, and treatment with IL-12 and IL-18 did not activate IFN-γ transcription in these cells (Fig. 3 A, left). iNKT cells that were transiently exposed to CD1d-transfected APCs alone showed only very little IFN-γ mRNA; however, subsequent treatment of these cells with IL-12 and IL-18 resulted in marked increases in IFN-γ mRNA (Fig. 3 A, left). By comparison, although rested iNKT cells also did not contain detectable levels of GM-CSF mRNA, transient exposure to CD1d-transfected APCs alone was sufficient to induce GM-CSF mRNA transcription, and subsequent

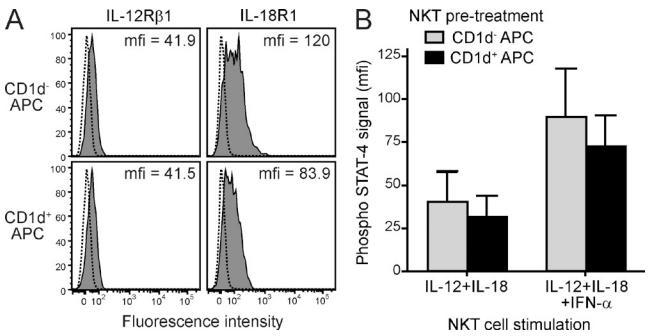

Figure 4. IL-12 and IL-18 receptor expression and STAT-4 signaling. (A) Cultured iNKT cells were rested by incubation in medium lacking IL-2, then exposed to CD1d⁻ or CD1d⁺ APCs, and stained with antibodies against IL-12Rβ1 or IL-18R1 (solid gray histograms), compared with isotype-matched negative control antibodies (dotted lines). Results are from one representative experiment out of two; similar results were also obtained in two independent experiments using a different iNKT cell clone. (B) Rested iNKT cells were preexposed to CD1d⁻ or CD1d⁺ APCs, then the APCs were removed, and the iNKT cells were stimulated with the cytokine mixtures shown on the x axis or left unstimulated. The iNKT cells were fixed, permeabilized, and analyzed by flow cytometry for intracellular levels of phospho–STAT-4. The plot shows the increase in the median phospho–STAT-4 signal in cytokine-treated iNKT cells compared with those incubated in medium alone. The bars show the means of four independent analyses on two different iNKT cell clones, with error bars showing the standard deviations. mfi, mean fluorescence intensity.

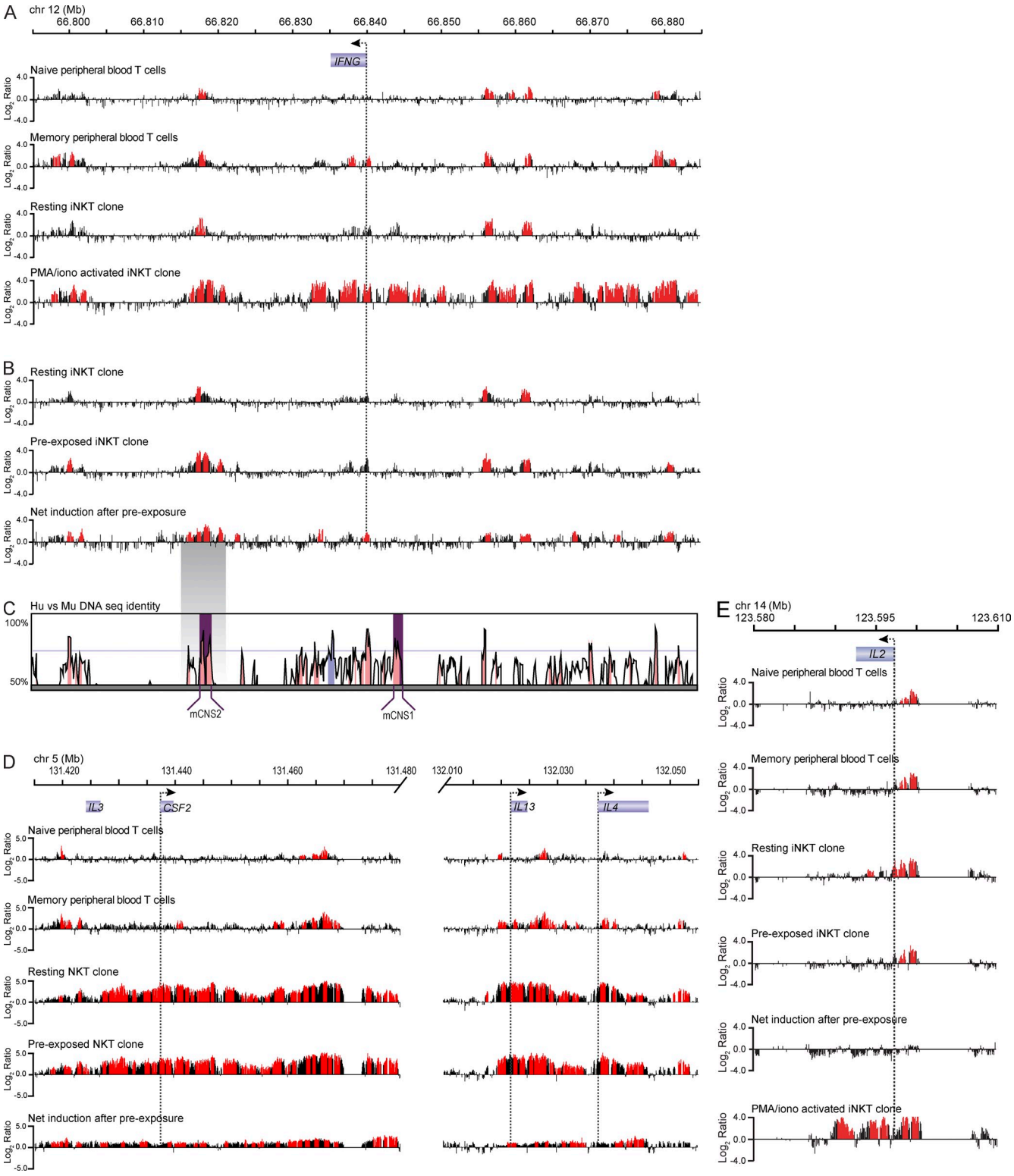

Figure 5. Induction of histone H4 acetylation at the *IFNG* locus. (A) Chromosomal DNA was prepared from naive or memory T cells isolated from human peripheral blood and from cells of a human iNKT clonal line that were either rested or stimulated with PMA and ionomycin and subject to ChIP-chip analysis of *IFNG* locus histone H4 acetylation. The tracks show $\log_2$ ratios of fluorescence from acetylated histone H4 immunoprecipitates compared with input DNA. Regions highlighted in red represent statistically significant signal (false discovery rate $P < 0.05$). Results shown are from a single analysis in which all of the samples were processed in parallel; similar results were obtained in two additional independent analyses. (B) Analysis of the *IFNG* locus of an iNKT clone that was rested (top track) compared with when it was exposed to $CD1d^+$ APCs for 4 h (middle track). Shown on the bottom track

exposure of the cells to IL-12 and IL-18 led to about a 50% further increase in the levels of GM-CSF mRNA (Fig. 3 A, right). The kinetics of IFN-γ mRNA induction after IL-12 and IL-18 exposure closely matched those of IFN-γ protein secretion (Fig. 3 B). Moreover, the ability to transcribe IFN-γ mRNA in response to IL-12 and IL-18 dropped off over time after removal of the CD1d-transfected APCs at a similar rate to what we had observed for IFN-γ secreted protein (Fig. 3 C). These results indicate that IL-12 and IL-18 cytokine stimulation activates gene transcription in iNKT cells, resulting in IFN-γ protein secretion; however, preexposure to $CD1d^+$ APCs is required for this to occur.

Mechanism of the priming effect

One potential explanation for the requirement for $CD1d^+$ APC exposure for iNKT cells to respond to IL-12 and IL-18 is that weak TCR stimulation leads to up-regulation of cytokine receptors on the iNKT cells. However, we found that the cell surface expression levels of the IL-12Rβ1 and IL-18R1 receptors did not appear to be up-regulated after antigenic stimulation of the iNKT cells (Fig. 4 A). We were not able to detect cell surface expression of the IL-12Rβ2 chain on our iNKT clones (not depicted). To further investigate, we tested the intracellular levels of phosphorylated STAT-4 in iNKT cells that were preexposed to $CD1d^-$ or $CD1d^+$ APCs and then stimulated by exposure to proinflammatory cytokines (i.e., either a mixture of IL-12 and IL-18 or a mixture of IL-12, IL-18, and IFN-α). Similar levels of STAT-4 phosphorylation were detected after cytokine exposure regardless of whether the iNKT cells had been preexposed to $CD1d^+$ APCs or not (Fig. 4 B). Thus, because autoantigenic stimulation does not appear to up-regulate IL-12 and IL-18 receptor expression or to enhance the ability of STAT-4 to become phosphorylated through agonism of these receptors, we hypothesized that its priming effect might be caused by a change in gene accessibility that enables JAK-STAT signaling to activate the transcription of IFN-γ mRNA.

Therefore, we investigated whether autoantigenic activation of iNKT cells produces epigenetic changes at the *IFNG* gene locus. We focused on histone acetylation because this type of modification often has a comparatively fast rate of turnover (Thomson et al., 2001), which would be consistent with our observation that the priming effect lasts only for a period of hours or days. We first compared the status of our iNKT clones to the naive and memory T cell subsets from freshly isolated human peripheral blood. Chromatin was immunoprecipitated (chromatin immunoprecipitation [ChIP]) using an antibody against acetylated histone H4 and then probed using a DNA microarray (chip). As shown in Fig. 5 A (first track), freshly isolated naive T cells had three main regions of histone H4 acetylation, at ∼40 kb upstream, 16–23 kb upstream, and 22 kb downstream of the *IFNG* transcriptional start site. Freshly isolated memory T cells also showed histone H4 acetylation signal at these sites, as well as in the immediate area of the *IFNG* gene and at a site ∼40 kb downstream (Fig. 5 A, second track). Remarkably, rested iNKT clones appeared more similar to the naive than the memory T cells subset (Fig. 5 A, third track). In contrast, after activation of the iNKT cells using PMA and ionomycin, the 40-kb and 22-kb downstream sites showed increased acetylation, and there was strong signal throughout the coding region and continuing upstream of the gene (Fig. 5 A, fourth track). Thus, the *IFNG* locus in iNKT cells is able to become heavily epigenetically modified upon strong activation, but the locus shows little histone H4 acetylation in rested iNKT cells.

We next performed a side by side comparison of rested iNKT cells with those that had been preexposed to CD1d-transfected APCs. In multiple independent experiments, we observed enhanced histone H4 acetylation signal in APC-preexposed iNKT cells at the 40-kb and 22-kb downstream sites, and there was also some increased signal in areas near the *IFNG* gene and at sites upstream (Fig. 5 B). By performing ChIP using anti–acetylated histone H4 or negative control antibodies followed by PCR using *IFNG* locus–specific primers, we confirmed that a similar effect occurred in another iNKT cell clone and in a polyclonal iNKT cell line (not depicted). In contrast to these effects of preexposure to $CD1d^+$ APCs on histone H4 acetylation levels in the *IFNG* locus, neither resting nor preexposed iNKT cells showed much signal for acetylation of lysine 9 on histone H3 at the *IFNG* locus (not depicted).

When we further analyzed these results, we found that the region of enhanced histone H4 acetylation that is ∼18–25 kb downstream of the *IFNG* transcription start site includes an area that has a high degree of sequence homology between mice and humans (Fig. 5 C). Located within this region of the mouse *IFNG* locus is a conserved noncoding sequence called CNS2 that has been found to be subject to transcriptionally favorable histone modifications in mice and to be able to enhance transcription of IFN-γ mRNA

is the net increase in acetylated histone H4 signal from the preexposed compared with the rested iNKT cells. Results shown are from one representative analysis out of three independent experiments. (C) mVista analysis of chromosomal sequence identity for this region of the human and mouse *IFNG* gene loci. Pink shaded areas indicate conserved noncoding sequences (CNS) identified by the mVista software, and blue shaded areas designate exons from the *IFNG* gene. The two areas highlighted in purple show regions that have been identified in the mouse *IFNG* gene locus as containing specific conserved noncoding sequences (mCNS1 or mCNS2) that have enhancer activity (Lee et al., 2004; Shnyreva et al., 2004). (D) ChIP-chip analysis of regions of chromosome 5 that contain genes encoding the cytokines IL-3 (*IL3*), GM-CSF (*CSF2*), IL-13 (*IL13*), and IL-4 (*IL4*). Results shown are from a single analysis in which all of the samples were processed in parallel; similar results were obtained in two additional independent analyses. (E) ChIP-chip analysis of the IL-2 locus. Results shown are from a single analysis in which all of the samples were processed in parallel; similar results were obtained in two additional independent analyses.

(Shnyreva et al., 2004). Moreover, this conserved noncoding sequence was recently found to be required for IFN-γ expression by human NKT cells (Collins et al., 2012). Thus, it seems likely that the epigenetic changes induced in this region by autoantigenic activation might facilitate later *IFNG* gene transcription in response to IL-12 and IL-18 receptor signaling.

For comparison, we also analyzed histone H4 acetylation at other cytokine gene loci. On chromosome 5, regions containing genes for GM-CSF (*CSF2*), IL-13 (*IL13*), and IL-4 (*IL4*) showed very strong signal in rested iNKT cells compared with freshly isolated peripheral blood T cells and underwent further acetylation after exposure to CD1d-transfected APCs (Fig. 5 D). In contrast, the *IL2* locus showed only one main region of histone H4 acetylation in rested iNKT cells, and there was no clear increase in the signal after exposure to CD1d-transfected APCs (Fig. 5 E). Importantly, however, the *IL2* locus of the iNKT cells was able to undergo histone H4 acetylation, as there was dense signal after activation by PMA and ionomycin (Fig. 5 E, right side). These observations highlight the distinctiveness of the basal and autoantigen-induced histone H4 acetylation patterns of iNKT cells. There is heavy acetylation in rested iNKT cells in regions of chromosome 5 that contain cytokine genes; however, the region of chromosome 12 surrounding the *IFNG* locus is comparatively unmodified in the same cells. Autoantigenic stimulation leads to increased histone H4 acetylation in discrete regions of the *IFNG* locus, but remarkably, this enhanced acetylation is not simply a ubiquitous effect because it does not occur at the *IL2* locus.

We next tested the impact of drugs that target enzymes involved in histone acetylation. Addition of an inhibitor that targets p300 (a histone acetyl transferase [HAT] enzyme that associates with a wide variety of transcription factors) during the exposure of NKT cells to $CD1d^+$ APCs produced a marked reduction in the amount of IFN-γ secreted in response to subsequent stimulation with IL-12 and IL-18, even though the drug was removed before the cytokine stimulation step (Fig. 6 A). Immunoprecipitation of chromosomal DNA fragments associated with acetylated histone H4 followed by PCR with primers specific for the 18–25 kb downstream site confirmed that treatment with the HAT inhibitor during exposure of iNKT cells to $CD1d^+$ APCs prevented the increase in acetylated histone H4 (Fig. 6 B). Together, these results suggest that histone H4 acetylation resulting from recognition of cell surface CD1d molecules is required for the ability of iNKT cells to subsequently secrete IFN-γ in response to IL-12 and IL-18.

Additionally, we found that the elevated levels of acetylated histone H4 in iNKT cells that had been exposed to $CD1d^+$ APCs decreased within 20 h to the levels observed in rested iNKT cells (Fig. 6 C). When iNKT cells that were preexposed to CD1d-transfected APCs were treated with the histone deacetylase (HDAC) inhibitor trichostatin A (TSA), a drug which inhibits the removal of acetyl groups from histones, then stimulated with IL-12 and IL-18 at varying time points after removal of the APCs, their ability to produce IFN-γ was prolonged from a half-time of 4.58 h to 7.95 h (Fig. 6 D). Importantly, treatment of rested iNKT cells with TSA did not result in significantly increased IFN-γ secretion in response to IL-12 and IL-18 stimulation (Fig. 6 E), indicating that this effect of the TSA was dependent on the prior stimulation from exposure to $CD1d^+$ APCs. Addition of TSA to freshly isolated human peripheral blood T cells that were depleted of $CD1d^+$ APCs also resulted in prolonged IL-12 and IL-18 responsiveness in the iNKT cell subset (Fig. 6 F). Thus, the decline in the innate responsiveness of autoantigen primed iNKT cells over time depends on the activity of HDAC enzymes. Together, these data support a mechanism in which autoantigen recognition by iNKT cells induces histone H4 acetylation at the *IFNG* locus that permits gene transcription in response to innate IL-12 and IL-18 signaling for the period of time until the acetylation is removed by HDAC enzymes.

Retention of motility during innate IFN-γ production

The finding that CD1d-mediated TCR stimulation of iNKT cells can be separated by a time delay from secretion of IFN-γ raises the question of whether the intervening time between these events can be used for migration away from the site of antigen recognition. We have previously demonstrated that in the absence of a strong TCR agonist, human iNKT cells make transient contacts with $CD1d^+$ APCs and retain their motility (Wang et al., 2008a), which is consistent with a previous report that in the absence of foreign antigens, mouse iNKT cells continuously traffic throughout the liver sinusoids despite the likelihood that they frequently encounter $CD1d^+$ APCs that may be presenting self-antigens (Geissmann et al., 2005). Thus, it seems likely that human iNKT cells that have been stimulated by autoantigen recognition are able to migrate to other sites. However, it remains unclear whether human iNKT cells continue to retain their motility after exposure to IL-12 and IL-18 because in one mouse model system this treatment induced migration arrest by iNKT cells in the liver (Velázquez et al., 2008).

We have previously observed that similar to stimulation by $CD1d^+$ APCs alone, iNKT cells that were stimulated by IL-12 and IL-18 in the presence of $CD1d^+$ APCs showed little cytoplasmic calcium flux, a critical part of the process by which T cells stop migrating and form stable conjugates with APCs (Wang et al., 2008a). To further investigate, we used microscopic and flow cytometric analyses to assess iNKT cell motility and interactions with myeloid APCs. iNKT cells were incubated with monocyte-derived human DCs in the presence of medium alone or medium containing IL-12 and IL-18 or after the DCs had been treated either with LPS or with α-GalCer, and time-lapse fluorescence microscopic photography was performed. Monocyte-derived DCs were used for these experiments instead of CD1d-transfected lymphoblastoid cell lines because the DCs would be more likely to modulate their expression of adhesion molecules during interactions with iNKT cells, and therefore they might be

more likely to induce iNKT cell migration stop. Tracking of the migration paths of individual iNKT cells revealed that iNKT cells showed similar migration distances regardless of whether they were incubated with DCs in the presence or absence of IL-12 and IL-18, as the distance migrated by each iNKT cell was typically >50 μm in a time span of 15 min (Fig. 7 A). iNKT cells that were incubated with LPS-treated DCs migrated similar distances as those exposed to DCs in the presence of IL-12 and IL-18 but exhibited more of a tethering pattern after contacting the DCs (Fig. 7 A and

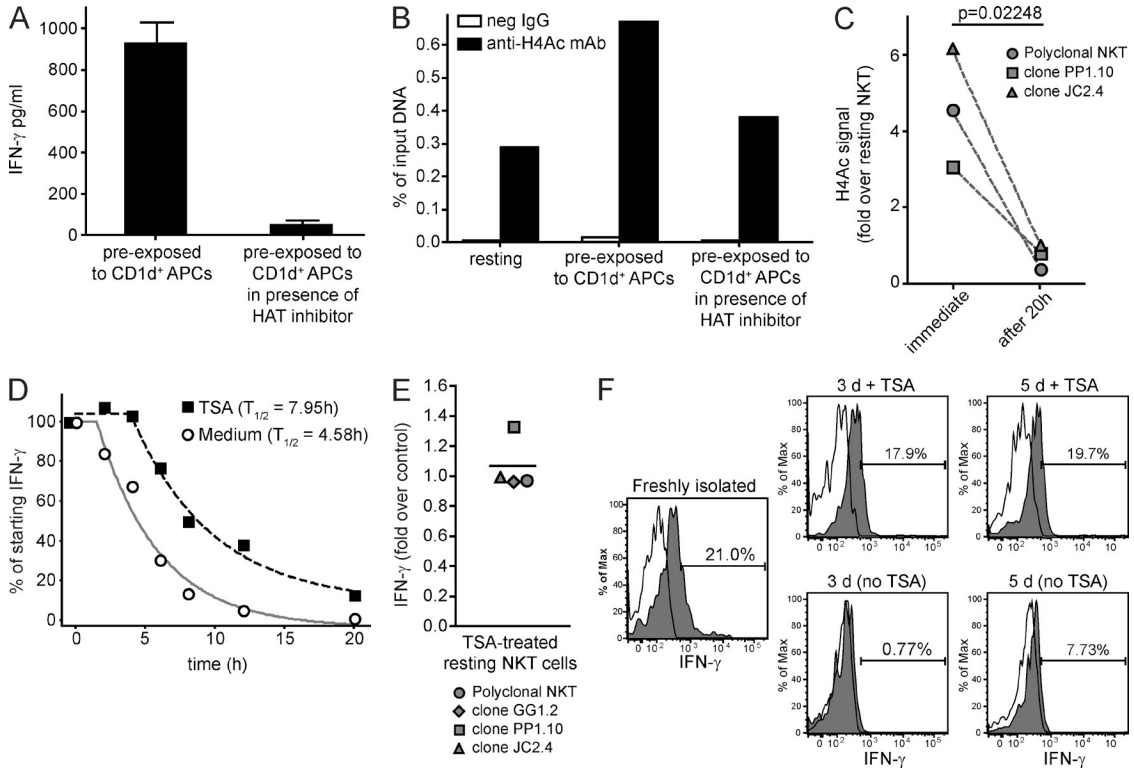

Figure 6. Dependence of IFN-γ production on histone acetylation. (A) Cultured iNKT cells were preexposed to CD1d+ APCs in the presence of vehicle alone or 11 μM HAT inhibitor dissolved in vehicle, then the APCs were removed, and the iNKT cells were washed and exposed to IL-12 and IL-18. IFN-γ secretion was measured by ELISA. The plot shows results from one representative experiment out of three; similar results were obtained in independent experiments using a different iNKT cell clone. Error bars indicate the standard deviations of the means. (B) Rested iNKT cells were left untreated (resting) or were exposed to CD1d+ APCs in the presence or absence of HAT inhibitor. The iNKT cells were fixed and lysed, and sheared chromatin was immunoprecipitated using an antibody against tetra-acetylated histone H4 (anti-H4Ac) or an isotype-matched negative control antibody (neg IgG), and the resulting purified DNA fragments were analyzed by quantitative PCR using primers that sit down in the region of the *IFNG* locus that is 18–25 kb downstream of the *IFNG* gene start site. Similar results were obtained with two additional primer pairs that localize to this region. (C) Compiled results from three independent experiments in which cultured iNKT cells were either preexposed to CD1d+ APCs or left untreated (resting). After removal of the APCs, the iNKT cells were either lysed immediately or after a 20-h incubation in culture medium. Immunoprecipitation was performed using an antibody against tetra-acetylated histone H4 (H4Ac) or with a negative control Ig, and PCR was performed using the same primers as in B. The PCR signals were normalized by the amount of input DNA for each condition, and the H4Ac enrichment was calculated by dividing the normalized signal from the H4Ac precipitate by that obtained from the negative control Ig precipitate. The plot shows the H4Ac enrichment from the indicated CD1d+ APC-pretreated iNKT cells as the fold over that obtained from the respective rested iNKT cells. Similar results were obtained in each case using a different set of primers that localize to this region. (D) Cultured iNKT cells were preexposed to CD1d-transfected APCs, then the APCs were removed, and the iNKT cells were incubated in the presence of medium alone or medium containing an HDAC inhibitor (TSA). After the indicated periods of time, IL-12 and IL-18 were added, and IFN-γ secretion was measured by ELISA. Results are expressed as the percentage of the amount produced when IL-12 and IL-18 were added immediately after removal of the APCs and are from one representative analysis out of three independent experiments. Similar results were obtained in three independent experiments on two additional iNKT cell clones. (E) Compiled results from four independent experiments in which rested iNKT cells were treated with TSA for 18 h or left untreated (control), and then the cells were washed and stimulated with IL-12 and IL-18, and secreted IFN-γ was quantitated by ELISA. The plot shows the amount of IFN-γ secreted by the indicated TSA-treated iNKT cells normalized by the amount secreted by the corresponding control iNKT cells. The horizontal bar indicates the mean. (F) Freshly isolated peripheral blood T cells depleted of CD1d+ cell populations were stimulated with IL-12, IL-18, and IFN-α and flow cytometrically analyzed for intracellular IFN-γ (dark gray histograms) compared with unstimulated cells (open histograms) or were incubated for 3 or 5 d in the presence or absence of the HDAC inhibitor TSA and then washed and similarly stimulated and analyzed for intracellular IFN-γ expression. Results are representative of four independent experiments performed using PBMCs isolated from two different donors.

Videos 1–4). In contrast, iNKT cells incubated with α-GalCer–pulsed DCs generally appeared almost stationary (Fig. 7 A). Analysis of the rate of migration showed that exposure to IL-12 and IL-18 produced a modest but statistically significant reduction in mean migration velocity compared with iNKT cells stimulated by autoantigen alone from a mean of 16.62 to 14.47 µm/min, but there was no significant further reduction in migration velocity in the presence of LPS-treated DCs (mean 13.96 µm/min), and exposure to α-GalCer–treated DCs produced a marked decrease in the mean iNKT cell migration velocity, to a mean of 6.15 µm/min (Fig. 7 B).

Flow cytometric analysis to quantitate the percentage of tightly adhered iNKT-DC conjugates revealed that whereas the addition of IL-12 and IL-18 did not produce a significant increase in conjugation, treatment of the DCs with LPS did result in significantly increased conjugation, although this was still less than the amount of iNKT cell conjugation observed with α-GalCer–pulsed DCs (Fig. 7 C). Similarly, microscopic analysis of fluorescently labeled iNKT cells incubated with monocyte-derived DCs revealed that after 2 h, the iNKT cells appeared to be almost completely co-clustered with α-GalCer–pulsed DCs, whereas iNKT cells incubated with unpulsed DCs in the presence or absence of added IL-12 and IL-18 showed little specific coclustering with the DCs (Fig. 7 D). Similar to the flow cytometric conjugation analysis, this microscopic assay suggested that the amount of co-clustering of iNKT cells with LPS-treated DCs was intermediate between that observed for α-GalCer–pulsed DCs and that observed for untreated DCs (Fig. 7 D). These results suggest that the presence of IL-12 and IL-18 in the local milieu slightly diminishes the speed of iNKT cell movement but does not induce migration stop. iNKT cells that encounter LPS-exposed DCs, which secrete proinflammatory cytokines and also express elevated levels of adhesion molecules, show increased DC interaction and may tend to be retained near the DCs, although they do not appear to undergo migration arrest. In contrast, when the iNKT cells are activated by a strong TCR signal (i.e., α-GalCer recognition), they undergo rapid migration arrest and form stable conjugates with DCs.

DISCUSSION

The results presented in this study demonstrate that although iNKT cells are able to produce IFN-γ in response to stimulation by IL-12 and IL-18 in the absence of a concurrent TCR signal (i.e., innately), this is not an intrinsic aspect of their differentiation state. Instead, the innate responsiveness of

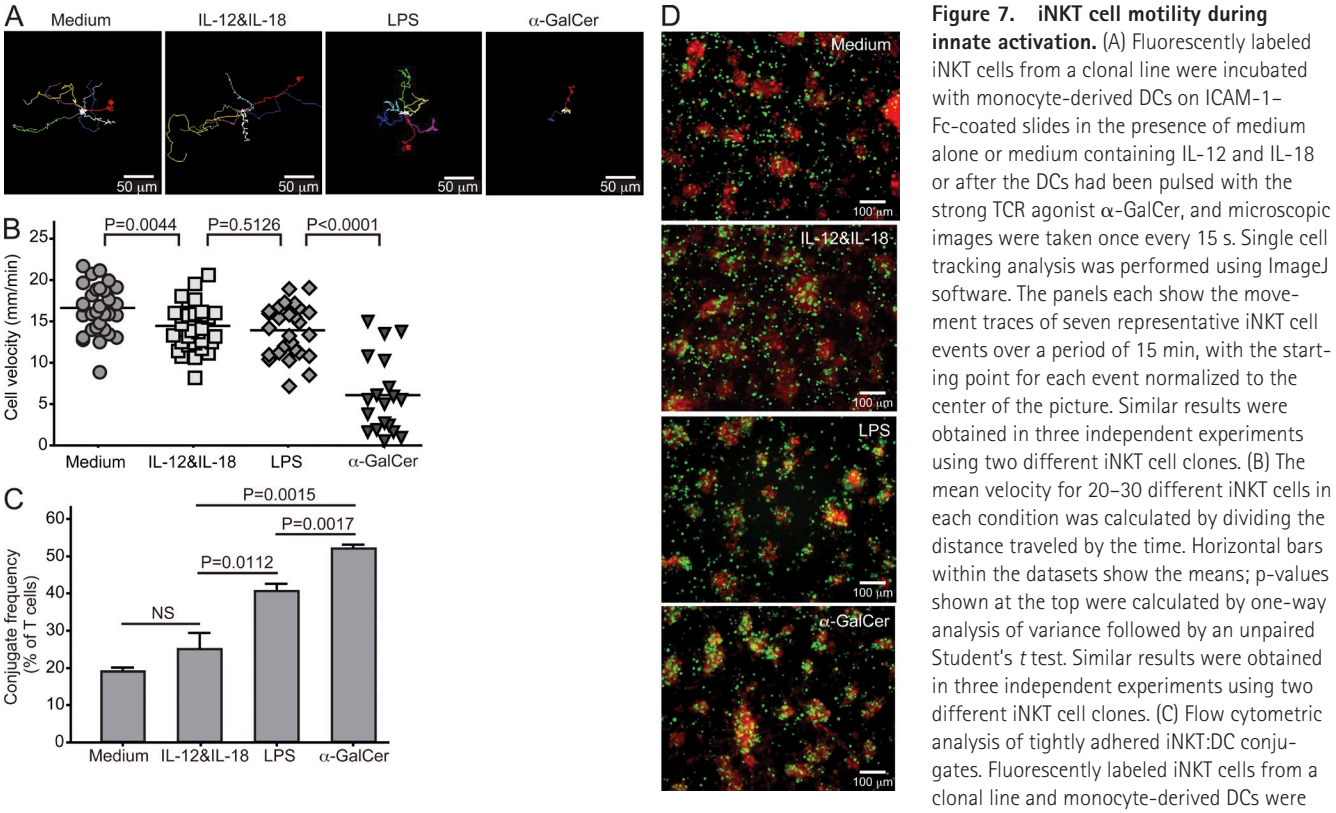

Figure 7. iNKT cell motility during innate activation. (A) Fluorescently labeled iNKT cells from a clonal line were incubated with monocyte-derived DCs on ICAM-1–Fc-coated slides in the presence of medium alone or medium containing IL-12 and IL-18 or after the DCs had been pulsed with the strong TCR agonist α-GalCer, and microscopic images were taken once every 15 s. Single cell tracking analysis was performed using ImageJ software. The panels each show the movement traces of seven representative iNKT cell events over a period of 15 min, with the starting point for each event normalized to the center of the picture. Similar results were obtained in three independent experiments using two different iNKT cell clones. (B) The mean velocity for 20–30 different iNKT cells in each condition was calculated by dividing the distance traveled by the time. Horizontal bars within the datasets show the means; p-values shown at the top were calculated by one-way analysis of variance followed by an unpaired Student's *t* test. Similar results were obtained in three independent experiments using two different iNKT cell clones. (C) Flow cytometric analysis of tightly adhered iNKT:DC conjugates. Fluorescently labeled iNKT cells from a clonal line and monocyte-derived DCs were coincubated for 24 h and then subjected to vigorous vortexing followed by flow cytometric analysis to determine the fraction of iNKT cells that had remained conjugated to the DCs. iNKT cells and untreated DCs were cultured in medium alone (medium) or in medium containing IL-12 and IL-18 (IL-12&IL-18), or iNKT cells were cultured with LPS-treated or α-GalCer–pulsed DCs as indicated. Each bar represents the mean conjugate frequency from three independent analyses, with error bars showing the standard deviations of the means. (D) Microscopic analysis of iNKT cells from a clonal line labeled with CFSE (green) incubated for 2 h with DCs labeled with DiD (red) under conditions corresponding to those described in C. Similar results were obtained in three independent experiments using two different iNKT cell clones.

iNKT cells is a transient condition that must be maintained by weak TCR stimulation, such as that resulting from the recognition of autoantigens presented by cell surface CD1d molecules. What is quite surprising is that iNKT cells display the ability to integrate these two qualitatively distinct signals, weak TCR stimulation and cytokine receptor signaling, across a time delay of hours or days. We show here for the first time that key to this ability is *IFNG* locus histone acetylation that is rapidly induced by weak TCR stimulation and then removed over the ensuing hours or days as a result of cellular HDAC enzyme activity.

Histone acetylation is a highly dynamic type of epigenetic modification that has been associated with increased accessibility of chromatin for gene transcription (Clayton et al., 2006). Whereas the acetylation of certain lysine residues on histone H3 tends to correlate with active gene transcription, the acetylation of histone H4 has been shown to correlate with areas of chromatin that are simply permissive or poised for gene transcription (Wang et al., 2008b). Previous analyses have found that resting NK cells and terminally differentiated T_{H1} cells have constitutively elevated histone H4 acetylation at specific chromosomal regions near the *IFNG* locus, suggesting that these cell types are epigenetically poised for IFN-γ production (Chang and Aune, 2005). Our results suggest that resting iNKT cells are poised for production of GM-CSF and IL-13 because the chromosomal regions containing these genes show nearly continuous histone H4 acetylation signal (Fig. 5 D). However, at least by this measure, resting iNKT cells do not appear highly predisposed toward IFN-γ production because their histone H4 acetylation pattern near the *IFNG* locus appears similar to that of naive peripheral blood T cells (Fig. 5 A). Thus, these results suggest that iNKT cells differ from NK cells and terminally differentiated T_{H1} cells in that their *IFNG* locus is not constitutively accessible, and consequently, innate IFN-γ production by iNKT cells requires that they have recently received a TCR stimulus to open up the gene locus.

Because human iNKT cells are able to recognize certain self-lipids (Fox et al., 2009; Brennan et al., 2011) and may also become activated by exogenous antigens that are abundant in the environment (Wingender et al., 2011), it seems likely that at any given time, some of the iNKT cells in vivo would be in this histone H4 poised state as a result of having recently received TCR stimulation. If so, this would explain our observation that a fraction of the iNKT cells within freshly isolated human PBMC samples are able to produce IFN-γ in an innate manner. Consistent with this, when we purified iNKT cells from human PBMCs directly ex vivo, the iNKT-enriched fraction showed ∼3.5-fold greater specific signal for acetylated histone H4 than the iNKT-depleted fraction from the same sample (unpublished data). However, a significant caveat for this type of experiment is that it is not currently possible to isolate or identify human iNKT cells without binding a reagent to the TCR. Because cross-linking of the TCR from this necessary step may induce histone acetylation, it is unclear whether the acetylation state of the ex vivo iNKT cells analyzed in this manner is representative of iNKT cells in vivo. Nevertheless, although this limits our ability to definitively determine the *IFNG* locus histone H4 acetylation states of primary human iNKT cells, we believe that the histone acetylation process we have delineated using cultured human iNKT cells provides a compelling explanation for the innate responses we observe from a fraction of the primary cells.

This mechanism may also explain previous observations that mouse iNKT cells were able to mediate antiviral IFN-γ responses in an innate manner even up to 1.5 d after they were adoptively transferred into CD1d-deficient mice (Tyznik et al., 2008; Wesley et al., 2008). In our experiments, using primary human peripheral blood lymphocytes, innate responsiveness was retained by a substantial fraction of the iNKT cells for at least 2–3 d after removal of $CD1d^+$ APCs. Thus, the primary iNKT cells appear to have a slower drop-off in innate responsiveness than cultured iNKT cells, which typically retained their responsiveness for only 12–16 h. The factors underlying this difference in decay kinetics are not yet clear; however, we speculate that it may be caused by a higher rate of HDAC activity in cultured iNKT cells compared with primary iNKT cells (presumably as a result of a higher overall metabolic rate in the cultured iNKT cells).

Although the mechanism of human iNKT cell innate reactivity delineated here is consistent with a substantial body of data demonstrating the functional autoreactivity of mouse iNKT cells in vivo (Bendelac et al., 2001; Kronenberg and Rudensky, 2005; Brigl and Brenner, 2010), it is important to note that our results do contrast somewhat with results from some of the previous studies performed in mouse model systems. It has recently been shown that mouse iNKT cells express very high levels of mRNA for both chains of the IL-12 receptor (Brennan et al., 2011). However, although we observed high cell surface expression of the IL-12Rβ1 chain on ex vivo human iNKT cells, we were not able to detect the IL-12Rβ2 chain on these cells using currently available commercial reagents. Therefore, it is possible that human and mouse iNKT cells have differences in IL-12 receptor expression, and correspondingly have different sensitivities to IL-12. Moreover, whereas in our experiments iNKT cells activated via the innate pathway demonstrated continued cellular motility, an analysis of the in vivo trafficking of mouse iNKT cells in the liver found that they underwent rapid migration arrest when they were exposed to IL-12 and IL-18 (Velázquez et al., 2008). The reason for this discrepancy is not clear, although as suggested by two recent analyses, it is possible that the liver provides distinctive signals not found in other tissues, or that it is an environment that provides for stronger adhesive interactions by innate lymphocytes such as iNKT cells that express high levels of the integrin LFA-1 (Thomas et al., 2011; Wong et al., 2011). Finally, an intriguing recent analysis that used transgenic mice expressing GFP as a TCR-signaling reporter gene revealed comparatively strong signaling in iNKT cells during thymic development but did not detect TCR signaling by iNKT cells in the periphery

(Moran et al., 2011). This finding calls into question the amount of autoantigenic TCR stimulation typically encountered by iNKT cells in peripheral tissues. However, it is not clear whether this result is actually an indication that mouse iNKT cells fail to undergo epigenetic modifications as a result of autoantigenic TCR stimulation because the TCR-dependent effects we observed did not result in gene transcription and thus might not be expected to result in the production of visible GFP in this reporter system.

The specific mechanism by which weak TCR stimulation induces histone H4 acetylation at the IFN-γ locus of iNKT cells also remains to be defined. Much of the work in this area thus far has focused on the processes leading to acetylation of histone H3, and less is known about histone H4. In genes that are actively undergoing transcription, histone H3 becomes hyperacetylated through highly dynamic processes (Lee and Mahadevan, 2009). The dynamic acetylation of histone H3 has recently been found to be mediated by p300/CBP acetyltransferases (Crump et al., 2011). The transcriptional co-activating functions of CBP are linked to AP-1, a transcription factor which is downstream of MAPK signaling (Bannister and Kouzarides, 1995). A role for MAPK signaling in the histone H4 acetylation we observed here would be consistent with our previous observation that autoantigenic stimulation of iNKT cells induces comparatively efficient ERK phosphorylation (Wang et al., 2008a), and the involvement of p300 in the acetylation effects that we observed would be consistent with our finding that the addition of a chemical compound to inhibit this enzyme during their exposure to $CD1d^+$ APCs prevents the iNKT cells from being able to subsequently respond to IL-12 and IL-18 (Fig. 6 A). However, we did not observe marked induction of histone H3 acetylation near the *IFNG* locus after autoantigenic stimulation of our iNKT cells (not depicted). Thus, because the MAPK–p300 pathway might also be expected to induce histone H3 acetylation, it is possible that distinct mechanisms are responsible for the histone H4 effects reported here.

The reversible mechanism of iNKT cell innate reactivity that we report here has significant clinical implications because the ability of iNKT cells to produce innate IFN-γ appears to be important for effective immunosurveillance of certain types of tumors and for their role in antimicrobial immune responses (Crowe et al., 2002; Brigl et al., 2003). Thus, defects in iNKT cell IFN-γ production such as those that have been observed in cancer patients (Tahir et al., 2001) might be related to dysregulation of this epigenetic priming pathway. It is also interesting to consider whether this activation process might occur in other types of innate T cells. This question may be of particular importance in humans because a population of human $CD4^+$ T cells has been found to resemble iNKT cells developmentally in that they are selected by antigen-presenting molecules that are expressed on other thymocytes, rather than by antigen-presenting molecules that are expressed by thymic epithelial cells (Li et al., 2005; Wei et al., 2005), and a variety of human peripheral blood T cell subsets representing >10% of the total PBMC have recently been shown to express the PLZF transcription factor, which confers innate-like properties in T cells (Eidson et al., 2011). Thus, it is possible that a substantial fraction of human T cells possess reversible epigenetic pathways of activation that are induced by weak TCR signaling, similar to what we have observed in iNKT cells. Given that weak TCR agonists are likely to be more abundant than strong ones, the results presented here suggest that it will be important to further investigate epigenetic changes that may result from seemingly nonproductive T cell signaling events.

MATERIALS AND METHODS

Analyses of IFN-γ production by human iNKT cells ex vivo. Protocols involving the collection and use of human tissues were approved by the University of Wisconsin Minimal Risk Institutional Review Board, and written informed consent was obtained from all blood donors. Human PBMCs were purified by density gradient centrifugation. Cells expressing CD14, CD19, CD304, CD141, and CD1c were depleted by magnetic sorting using an AutoMACS system (Miltenyi Biotec). The remaining cells were incubated in culture medium alone or in culture medium containing 5 U/ml IL-12, 50 ng/ml IL-18, and 5×10^4 U/ml IFN-α for 14 h. The cells were stained with anti-CD3 and α-GalCer–loaded human CD1d tetramers to identify the iNKT cell subset and then stained intracellularly with anti–IFN-γ or a negative control antibody and analyzed by flow cytometry.

iNKT cell clones and APCs. Human CD1d-restricted iNKT cell clones were generated and maintained as described previously (Brigl et al., 2006). iNKT cells were incubated in culture medium lacking IL-2 for 18–24 h before all stimulation assays to ensure a fully rested state, and assays were performed in medium lacking IL-2. CD1d transfectants were generated from the 3023 human lymphoblastoid cell line as described previously (Chen et al., 2007). Monocyte-derived DCs were prepared by culturing freshly isolated human peripheral blood monocytes (purified by magnetic sorting of $CD14^+$ cells) for 3–4 d in culture medium (RPMI 1640 medium supplemented with 2 mM L-glutamine, 100 μg/ml penicillin and streptomycin, and 10% fetal bovine serum) containing 300 U/ml GM-CSF or 300 U/ml GM-CSF and 400 U/ml IL-4.

iNKT cell stimulation. CD1d-transfected or $CD1d^-$ 3023 cells were surface labeled with NHS-biotin (Thermo Fisher Scientific) and then incubated with iNKT cells for 4 h. Where indicated, the MEK inhibitor U0126, the calcium signaling inhibitor CsA, the p300 acetyltransferase inhibitor HAT inhibitor II, or the HDAC inhibitor TSA (all from EMD) were included in the co-culture. The APCs were removed by magnetic sorting using anti-biotin beads (Miltenyi Biotec). Flow cytometric analysis confirmed that the APC-depleted iNKT cell population was >99.5% pure (Wang et al., 2008a). The purified iNKT cells were incubated in medium with or without 5 U/ml IL-12 and 50 ng/ml IL-18 in the presence of a 1:1 ratio of $CD1d^-$ 3023 cells. Where indicated, inhibitors were added to the iNKT cells during the IL-12 and IL-18 exposure step (e.g., U0126, CsA, the p38 kinase inhibitors SB203580 or SB202190, or the inactive analogue SB202474). Where indicated, APCs were pulsed with 50 ng/ml of synthetic α-GalCer that was provided by G.S. Besra (University of Birmingham, Birmingham, England, UK) and was prepared as described previously (Yu et al., 2005).

mRNA quantification. iNKT cells were preexposed to CD1d-transfected or $CD1d^-$ 3023 cells, and mRNA was prepared by guanidine-isothiocyanate lysis followed by silica adsorption (QIAGEN). The purified RNA was reverse transcribed using a first strand cDNA synthesis kit (Roche), and real-time PCR was performed using primers for IFN-γ (5′-TTCCTTGATGGTCTCCACAC-3′ and 5′-GAATTGGAAAGAGGAGAGTGA-3′), β-actin (5′-TAGCACAGCCTGGATAGCAAC-3′ and 5′-CATCGAGCACGGCATCGTCA-3′), or GM-CSF (5′-TACAGACCCGCCTGGAGC-3′ and 5′-ATAATCTGGGTTGCACAGGAA-3′).

Analysis of IL-12R and IL-18R cell surface expression and STAT-4 phosphorylation. Resting or prestimulated iNKT clonal lines were stained using antibodies against IL-12Rβ1 or IL-12Rβ2 (BD) or IL-18R (BioLegend) and then analyzed by flow cytometry. For analysis of STAT-4 phosphorylation, iNKT cells were preexposed to biotinylated CD1d-transfected or $CD1d^-$ 3023 cells, then the APCs were removed, and the iNKT cells were fixed with methanol, washed, and incubated with a polyclonal rabbit antibody against phospho–STAT-4 (phospho-Y693; R&D Systems) or with nonimmune rabbit serum, followed by staining with goat anti–rabbit antibody labeled with Alexa Fluor 488 (Invitrogen).

ChIP-microarray analysis. ChIP analysis was performed as described previously (Bishop et al., 2009) using an antibody specific for acetylated histone H4 (6-866; Millipore) or a negative control rabbit IgG antibody. Immunoprecipitated DNA was blunt-ended by T4 DNA Polymerase, ligated to linkers with the sequences 5′-GAATTCAGATC-3′ and 5′-GCGGTGACCCGGGAGATCTGAATTC-3′ using T4 DNA ligase, and amplified by ligation-mediated PCR. Purified PCR products were labeled with Cy3 or Cy5 9-mer wobble primers using Klenow fragment, and labeled DNA samples were co-hybridized to a custom oligonucleotide microarray (synthesized by Roche) using a NimbleGen Hybridization kit (Roche) and a MAUI hybridization system (BioMicro Systems, Inc.). Microarrays were scanned using an Axon 4000B scanner with GenepixPro version 4.1 software (Molecular Devices). The microarray oligonucleotide probes were 50–70 mer in length with 68-bp resolution and synthesized using a mask-less array system tiled from ∼190 kb upstream of the *IFNG* TSS to ∼300 kb downstream of the final 3′ coding exon. NimbleScan version 1.9.0.05 software (Roche) was used for statistical analysis of data. A sliding window of 700 bp containing at least four out of eight probes statistically above background was deemed significant. To further analyze the data, gene sequences surrounding the human *IFNG* (chr12, 66.790–66.890 Mb) and mouse *Ifng* gene (chr10, 117.750–117.950 Mb) were aligned using the mVista algorithm (Mayor et al., 2000; Frazer et al., 2004). Sequences from the mouse CNS1 and CNS2 that were conserved in corresponding parts of the human chromosome were identified and annotated at the human *IFNG* gene locus.

Real-time PCR analysis. DNA immunoprecipitated using an anti–acetylated histone H4 (6-866) antibody or a negative control rabbit IgG antibody was tested by real-time PCR for the presence of fragments from the *IFNG* locus. Primer pairs used for the analysis included the following: IFNG ChIP 66816016–6681616, 5′-GCTGGGTCAGCCAGGAGGTTAGAG-3′ (forward) and 5′-TGTCTACCCTGGACCCCTCAGTGT-3′ (reverse); IFNG ChIP 66818603–66818752, 5′-GCCGGTGTTACATTGTCCTGGTGT-3′ (forward) and 5′-GGCTCAGGAGTTAGGAAATCCCCA-3′ (reverse); IFNG ChIP 66820288–66820397, 5′-TTGGTCCTGTTCTTGCTCCTCCCA-3′ (forward) and 5′-ACAGGGGAAAGTGTAGTACGCTGA-3′ (reverse); and IFNG 66880057–66880255, 5′-GAAGGGCTGAGAAACATTC-3′ (forward) and 5′-CCTCTATTGCTCCTGACTGA-3′. Standard curves were made by serial dilutions of ChIP input DNA. Experiments were performed on a Realplex (Eppendorf) using Power SYBR Green PCR Master Mix or FastStart SYBR Green Mast (Roche) with standard cycling conditions. Mastercycler ep Realplex software (Eppendorf) was used for analysis.

Time-lapse microscopy of iNKT cell migration. Poly-L-lysine–coated slides (Polysciences) were coated with human ICAM-1–Fc fusion protein (a gift of L. Klickstein, Brigham and Women's Hospital, Boston, MA) and blocked with BSA in PBS. Monocyte-derived DCs and cultured human iNKT cells were labeled with DiD and CFSE, respectively (Invitrogen). Microscopic analysis was performed on a Radiance 2100 MP Rainbow confocal system (Bio-Rad Laboratories). Videos were made by taking photographic images at 15-s intervals for a period of 40–60 min. Single cell tracking analysis was performed using ImageJ software (National Institutes of Health). Migration speed was determined by dividing the distance migrated by each T cell by the total time of analysis.

Online supplemental material. Videos 1–4 are time-lapse videos showing fluorescently labeled cultured human iNKT cells migrating and interacting with LPS-matured monocyte-derived DCs on slides coated with recombinant ICAM-1. Online supplemental material is available at http://www.jem.org/cgi/content/full/jem.20111024/DC1.

Funding for this work was provided by National Institutes of Health grants R01 AI060777 and R01 AI074940 to J.E. Gumperz. The funders had no role in study design, data collection and analysis, decision to publish, or preparation of the manuscript.

The authors have no competing financial interests.

Submitted: 20 May 2011
Accepted: 30 March 2012

REFERENCES

Bannister, A.J., and T. Kouzarides. 1995. CBP-induced stimulation of c-Fos activity is abrogated by E1A. *EMBO J.* 14:4758–4762.

Bendelac, A., M. Bonneville, and J.F. Kearney. 2001. Autoreactivity by design: innate B and T lymphocytes. *Nat. Rev. Immunol.* 1:177–186. http://dx.doi.org/10.1038/35105052

Bishop, K.A., M.B. Meyer, and J.W. Pike. 2009. A novel distal enhancer mediates cytokine induction of mouse RANKl gene expression. *Mol. Endocrinol.* 23:2095–2110. http://dx.doi.org/10.1210/me.2009-0209

Brennan, P.J., R.V. Tatituri, M. Brigl, E.Y. Kim, A. Tuli, J.P. Sanderson, S.D. Gadola, F.F. Hsu, G.S. Besra, and M.B. Brenner. 2011. Invariant natural killer T cells recognize lipid self antigen induced by microbial danger signals. *Nat. Immunol.* 12:1202–1211. http://dx.doi.org/10.1038/ni.2143

Brigl, M., and M.B. Brenner. 2010. How invariant natural killer T cells respond to infection by recognizing microbial or endogenous lipid antigens. *Semin. Immunol.* 22:79–86. http://dx.doi.org/10.1016/j.smim.2009.10.006

Brigl, M., L. Bry, S.C. Kent, J.E. Gumperz, and M.B. Brenner. 2003. Mechanism of CD1d-restricted natural killer T cell activation during microbial infection. *Nat. Immunol.* 4:1230–1237. http://dx.doi.org/10.1038/ni1002

Brigl, M., P. van den Elzen, X. Chen, J.H. Meyers, D. Wu, C.H. Wong, F. Reddington, P.A. Illarianov, G.S. Besra, M.B. Brenner, and J.E. Gumperz. 2006. Conserved and heterogeneous lipid antigen specificities of CD1d-restricted NKT cell receptors. *J. Immunol.* 176:3625–3634.

Brigl, M., R.V. Tatituri, G.F. Watts, V. Bhowruth, E.A. Leadbetter, N. Barton, N.R. Cohen, F.F. Hsu, G.S. Besra, and M.B. Brenner. 2011. Innate and cytokine-driven signals, rather than microbial antigens, dominate in natural killer T cell activation during microbial infection. *J. Exp. Med.* 208:1163–1177. http://dx.doi.org/10.1084/jem.20102555

Chang, S., and T.M. Aune. 2005. Histone hyperacetylated domains across the Ifng gene region in natural killer cells and T cells. *Proc. Natl. Acad. Sci. USA.* 102:17095–17100. http://dx.doi.org/10.1073/pnas.0502129102

Chen, X., X. Wang, J.M. Keaton, F. Reddington, P.A. Illarionov, G.S. Besra, and J.E. Gumperz. 2007. Distinct endosomal trafficking requirements for presentation of autoantigens and exogenous lipids by human CD1d molecules. *J. Immunol.* 178:6181–6190.

Clayton, A.L., C.A. Hazzalin, and L.C. Mahadevan. 2006. Enhanced histone acetylation and transcription: a dynamic perspective. *Mol. Cell.* 23:289–296. http://dx.doi.org/10.1016/j.molcel.2006.06.017

Collins, P.L., M.A. Henderson, and T.M. Aune. 2012. Diverse functions of distal regulatory elements at the IFNG locus. *J. Immunol.* 188:1726–1733. http://dx.doi.org/10.4049/jimmunol.1102879

Cox, D., L. Fox, R. Tian, W. Bardet, M. Skaley, D. Mojsilovic, J. Gumperz, and W. Hildebrand. 2009. Determination of cellular lipids bound to human CD1d molecules. *PLoS ONE.* 4:e5325. http://dx.doi.org/10.1371/journal.pone.0005325

Crowe, N.Y., M.J. Smyth, and D.I. Godfrey. 2002. A critical role for natural killer T cells in immunosurveillance of methylcholanthrene-induced sarcomas. *J. Exp. Med.* 196:119–127. http://dx.doi.org/10.1084/jem.20020092

Crump, N.T., C.A. Hazzalin, E.M. Bowers, R.M. Alani, P.A. Cole, and L.C. Mahadevan. 2011. Dynamic acetylation of all lysine-4 trimethylated histone H3 is evolutionarily conserved and mediated by p300/CBP. *Proc. Natl. Acad. Sci. USA*. 108:7814–7819. http://dx.doi.org/10.1073/pnas.1100099108

Eidson, M., J. Wahlstrom, A.M. Beaulieu, B. Zaidi, S.E. Carsons, P.K. Crow, J. Yuan, J.D. Wolchok, B. Horsthemke, D. Wieczorek, and D.B. Sant'Angelo. 2011. Altered development of NKT cells, γδ T cells, CD8 T cells and NK cells in a PLZF deficient patient. *PLoS ONE*. 6:e24441. http://dx.doi.org/10.1371/journal.pone.0024441

Fitzpatrick, D.R., and C.B. Wilson. 2003. Methylation and demethylation in the regulation of genes, cells, and responses in the immune system. *Clin. Immunol.* 109:37–45. http://dx.doi.org/10.1016/S1521-6616(03)00205-5

Fox, L.M., D.G. Cox, J.L. Lockridge, X. Wang, X. Chen, L. Scharf, D.L. Trott, R.M. Ndonye, N. Veerapen, G.S. Besra, et al. 2009. Recognition of lyso-phospholipids by human natural killer T lymphocytes. *PLoS Biol.* 7:e1000228. http://dx.doi.org/10.1371/journal.pbio.1000228

Frazer, K.A., L. Pachter, A. Poliakov, E.M. Rubin, and I. Dubchak. 2004. VISTA: computational tools for comparative genomics. *Nucleic Acids Res.* 32:W273–W279. http://dx.doi.org/10.1093/nar/gkh458

Geissmann, F., T.O. Cameron, S. Sidobre, N. Manlongat, M. Kronenberg, M.J. Briskin, M.L. Dustin, and D.R. Littman. 2005. Intravascular immune surveillance by CXCR6+ NKT cells patrolling liver sinusoids. *PLoS Biol.* 3:e113. http://dx.doi.org/10.1371/journal.pbio.0030113

Kawano, T., J. Cui, Y. Koezuka, I. Toura, Y. Kaneko, K. Motoki, H. Ueno, R. Nakagawa, H. Sato, E. Kondo, et al. 1997. CD1d-restricted and TCR-mediated activation of valpha14 NKT cells by glycosylceramides. *Science*. 278:1626–1629. http://dx.doi.org/10.1126/science.278.5343.1626

Kinjo, Y., D. Wu, G. Kim, G.W. Xing, M.A. Poles, D.D. Ho, M. Tsuji, K. Kawahara, C.H. Wong, and M. Kronenberg. 2005. Recognition of bacterial glycosphingolipids by natural killer T cells. *Nature*. 434:520–525. http://dx.doi.org/10.1038/nature03407

Kronenberg, M., and A. Rudensky. 2005. Regulation of immunity by self-reactive T cells. *Nature*. 435:598–604. http://dx.doi.org/10.1038/nature03725

Lee, B.M., and L.C. Mahadevan. 2009. Stability of histone modifications across mammalian genomes: implications for 'epigenetic' marking. *J. Cell. Biochem.* 108:22–34. http://dx.doi.org/10.1002/jcb.22250

Lee, D.U., O. Avni, L. Chen, and A. Rao. 2004. A distal enhancer in the interferon-gamma (IFN-gamma) locus revealed by genome sequence comparison. *J. Biol. Chem.* 279:4802–4810. http://dx.doi.org/10.1074/jbc.M307904200

Li, W., M.G. Kim, T.S. Gourley, B.P. McCarthy, D.B. Sant'Angelo, and C.H. Chang. 2005. An alternate pathway for CD4 T cell development: thymocyte-expressed MHC class II selects a distinct T cell population. *Immunity*. 23:375–386. http://dx.doi.org/10.1016/j.immuni.2005.09.002

Mattner, J., K.L. Debord, N. Ismail, R.D. Goff, C. Cantu III, D. Zhou, P. Saint-Mezard, V. Wang, Y. Gao, N. Yin, et al. 2005. Exogenous and endogenous glycolipid antigens activate NKT cells during microbial infections. *Nature*. 434:525–529. http://dx.doi.org/10.1038/nature03408

Mayor, C., M. Brudno, J.R. Schwartz, A. Poliakov, E.M. Rubin, K.A. Frazer, L.S. Pachter, and I. Dubchak. 2000. VISTA: visualizing global DNA sequence alignments of arbitrary length. *Bioinformatics*. 16:1046–1047. http://dx.doi.org/10.1093/bioinformatics/16.11.1046

Moran, A.E., K.L. Holzapfel, Y. Xing, N.R. Cunningham, J.S. Maltzman, J. Punt, and K.A. Hogquist. 2011. T cell receptor signal strength in T_{reg} and iNKT cell development demonstrated by a novel fluorescent reporter mouse. *J. Exp. Med.* 208:1279–1289. http://dx.doi.org/10.1084/jem.20110308

Nagarajan, N.A., and M. Kronenberg. 2007. Invariant NKT cells amplify the innate immune response to lipopolysaccharide. *J. Immunol.* 178:2706–2713.

Reiner, S.L., A.C. Mullen, A.S. Hutchins, and E.L. Pearce. 2003. Helper T cell differentiation and the problem of cellular inheritance. *Immunol. Res.* 27:463–468. http://dx.doi.org/10.1385/IR:27:2-3:463

Shnyreva, M., W.M. Weaver, M. Blanchette, S.L. Taylor, M. Tompa, D.R. Fitzpatrick, and C.B. Wilson. 2004. Evolutionarily conserved sequence elements that positively regulate IFN-gamma expression in T cells. *Proc. Natl. Acad. Sci. USA*. 101:12622–12627. http://dx.doi.org/10.1073/pnas.0400849101

Stetson, D.B., M. Mohrs, R.L. Reinhardt, J.L. Baron, Z.E. Wang, L. Gapin, M. Kronenberg, and R.M. Locksley. 2003. Constitutive cytokine mRNAs mark natural killer (NK) and NK T cells poised for rapid effector function. *J. Exp. Med.* 198:1069–1076. http://dx.doi.org/10.1084/jem.20030630

Tahir, S.M., O. Cheng, A. Shaulov, Y. Koezuka, G.J. Bubley, S.B. Wilson, S.P. Balk, and M.A. Exley. 2001. Loss of IFN-gamma production by invariant NK T cells in advanced cancer. *J. Immunol.* 167:4046–4050.

Thomas, S.Y., S.T. Scanlon, K.G. Griewank, M.G. Constantinides, A.K. Savage, K.A. Barr, F. Meng, A.D. Luster, and A. Bendelac. 2011. PLZF induces an intravascular surveillance program mediated by long-lived LFA-1–ICAM-1 interactions. *J. Exp. Med.* 208:1179–1188. http://dx.doi.org/10.1084/jem.20102630

Thomson, S., A.L. Clayton, and L.C. Mahadevan. 2001. Independent dynamic regulation of histone phosphorylation and acetylation during immediate-early gene induction. *Mol. Cell.* 8:1231–1241. http://dx.doi.org/10.1016/S1097-2765(01)00404-X

Tyznik, A.J., E. Tupin, N.A. Nagarajan, M.J. Her, C.A. Benedict, and M. Kronenberg. 2008. Cutting edge: the mechanism of invariant NKT cell responses to viral danger signals. *J. Immunol.* 181:4452–4456.

Velázquez, P., T.O. Cameron, Y. Kinjo, N. Nagarajan, M. Kronenberg, and M.L. Dustin. 2008. Cutting edge: activation by innate cytokines or microbial antigens can cause arrest of natural killer T cell patrolling of liver sinusoids. *J. Immunol.* 180:2024–2028.

Wang, X., X. Chen, L. Rodenkirch, W. Simonson, S. Wernimont, R.M. Ndonye, N. Veerapen, D. Gibson, A.R. Howell, G.S. Besra, et al. 2008a. Natural killer T-cell autoreactivity leads to a specialized activation state. *Blood*. 112:4128–4138. http://dx.doi.org/10.1182/blood-2008-05-157529

Wang, Z., C. Zang, J.A. Rosenfeld, D.E. Schones, A. Barski, S. Cuddapah, K. Cui, T.Y. Roh, W. Peng, M.Q. Zhang, and K. Zhao. 2008b. Combinatorial patterns of histone acetylations and methylations in the human genome. *Nat. Genet.* 40:897–903. http://dx.doi.org/10.1038/ng.154

Wei, D.G., H. Lee, S.H. Park, L. Beaudoin, L. Teyton, A. Lehuen, and A. Bendelac. 2005. Expansion and long-range differentiation of the NKT cell lineage in mice expressing CD1d exclusively on cortical thymocytes. *J. Exp. Med.* 202:239–248. http://dx.doi.org/10.1084/jem.20050413

Wesley, J.D., M.S. Tessmer, D. Chaukos, and L. Brossay. 2008. NK cell-like behavior of Valpha14i NK T cells during MCMV infection. *PLoS Pathog.* 4:e1000106. http://dx.doi.org/10.1371/journal.ppat.1000106

Wingender, G., P. Rogers, G. Batzer, M.S. Lee, D. Bai, B. Pei, A. Khurana, M. Kronenberg, and A.A. Horner. 2011. Invariant NKT cells are required for airway inflammation induced by environmental antigens. *J. Exp. Med.* 208:1151–1162. http://dx.doi.org/10.1084/jem.20102229

Wong, C.H., C.N. Jenne, W.Y. Lee, C. Léger, and P. Kubes. 2011. Functional innervation of hepatic iNKT cells is immunosuppressive following stroke. *Science*. 334:101–105. http://dx.doi.org/10.1126/science.1210301

Yang, J., H. Zhu, T.L. Murphy, W. Ouyang, and K.M. Murphy. 2001. IL-18-stimulated GADD45 beta required in cytokine-induced, but not TCR-induced, IFN-gamma production. *Nat. Immunol.* 2:157–164. http://dx.doi.org/10.1038/84264

Yu, K.O., J.S. Im, A. Molano, Y. Dutronc, P.A. Illarionov, C. Forestier, N. Fujiwara, I. Arias, S. Miyake, T. Yamamura, et al. 2005. Modulation of CD1d-restricted NKT cell responses by using N-acyl variants of alpha-galactosylceramides. *Proc. Natl. Acad. Sci. USA*. 102:3383–3388. http://dx.doi.org/10.1073/pnas.0407488102

Yuan, W., S.J. Kang, J.E. Evans, and P. Cresswell. 2009. Natural lipid ligands associated with human CD1d targeted to different subcellular compartments. *J. Immunol.* 182:4784–4791. http://dx.doi.org/10.4049/jimmunol.0803981